DESIGN AND IMPLEMENTATION OF LITHIUM ION BATTERY CHARGER

[1*]Yusuf,Y.[2]Bello, M.,[2]Abdulmuminu, I. and [3]Yahya, H.N.
[1]*Department of Physics, Zamfara College of Arts and Science, Gusau, Nigeria*
[2]*Department of Physics, Federal University, Gusau, Zamfara State, Nigeria*
[3]*Department of Electrical and Electronics, Usmanu Danfodio University, Sokoto, Nigeria*
*Corresponding author email: bazata70@gmail.com

ABSTRACT

Although most modern electrical equipment receives power directly from the wall socket, there are number of equipment that requires electrical power from storage batteries for effective performance and convenience. Lithium battery stores electricity from the national grid for later use and can be recharged conveniently when its energy has been drained. There are many electrical appliances that use this type of battery. This paper deals with the design and implementation of an alternating current (AC) to direct current (DC) to charge a lithium ion battery. A self-oscillation fly back switch mode power supply (SMPS) topology was adopted. The circuit components and other design materials were chosen based on simplicity and availability within the locality. The green light emitting diode (LED) is ON when charging is completed. MULTISIM software was used in design before implementation procedure. The construction was first done on the separate breadboard later transferred to the Vero-board. The components were soldered one after the other on their positions. Continuity tests were also conducted to ensure that the joints were properly done. Performance analysis was later carried out and found working applicably.

Alternating Current, Direct Current, Switched Mode Power Supply, Light Emitting Diode

INTRODUCTION

A battery charger or recharger is a device used to put energy into a secondary cell or rechargeable battery by forcing an electric current through it (Odia and Okpor, 2017). Almost all Portable electronic devices are battery powered; eventually they all must be charged using the wired chargers (Joe *et al.*, 2018). Christine (2011) shows that, a current-limited power supply maintains a constant voltage across the battery (approximately 2.4V/cell, as specified by the battery manufacturer) until the charging current decreases below a current threshold defined by the capacity of the battery. At this point, the charger is placed in a trickle-charge mode. Although, switch mode power supply is much complicated than regulated power supply, it has advantages of being smaller size, lighter weight and a greater efficiency. This is because the switching transistor dissipates little power in the saturated state and the off state compared to the active region. Udezue *et al.* (2016) Observed that irrespective of the level of discharge, most battery service centres often connect the batteries and allow them to charge without a means to automatically disconnect them when they are fully charged in order to prevent over-charge and possible explosion. Ovbiagele, U. and Jerome, D. K., (2017) have designed and implemented a 12 V automatic battery charger using adjustable voltage regulator LM317T integrated circuit.Francisco,*et al* (2019) has also designed and constructed a multi-purpose hand crank mechanical energy charger. In this study single fly back switch mode power supply circuit is designed for charging a lithium battery from the (AC) mains power supply. To minimise the risk of damage due to overcharging, a fully charge indicator is added. Green LED indicator is ON to show that the charging is completed. It is designed to operate on universal input voltage range of 85 V AC to 265 V AC.

Basic Switch Mode Power Supply

Switched mode power supply (SMPS) can be a fairly complicated circuit, as can be seen from the block diagram shown in Figure 1(This configuration assumes a 50/60Hz mains input supply is used). The AC supply is first rectified, and then filtered by the input reservoir capacitor to produce a rough DC input supply. This level can fluctuate widely due to variations in the mains. In addition the capacitance on the input has to be fairly large to hold up the supply in case of a severe drop in the mains (Humphreys*et al.*, 1994).

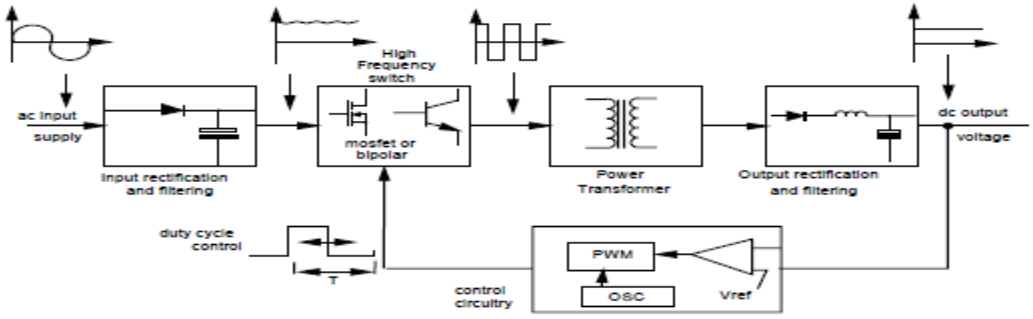

Figure 1: Basic switched mode power supply block diagram (Humphreys*et al.*, 1994)

Alex, (2008) AC to DC power supplies combine a transformer isolated DC-DC converter with an AC rectifier circuit that includes diodes (rectifiers), a filter capacitor, and optionally a power factor correction circuit. Fly back converters are low cost designs typically used for low power applications (5-150 watts). Fly back converters also do not require output inductors which save cost (Figure 2).

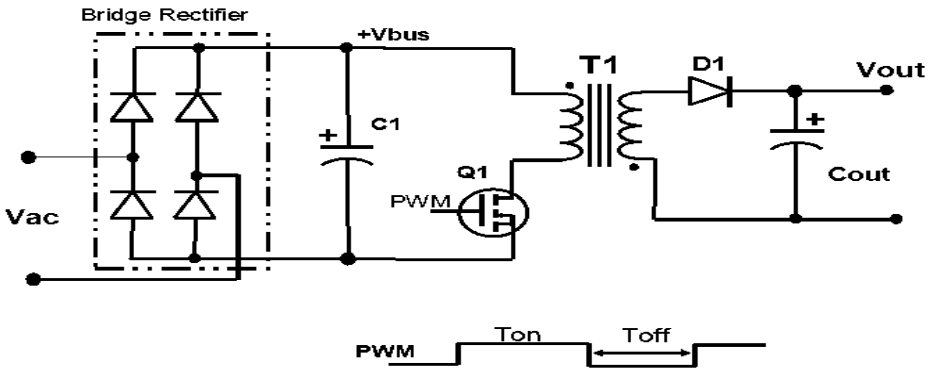

Figure 2: Fly back AC to DC converter (Alex, 2008)

The Fly-back converter uses the transformer as an energy storage device as well as an energy transfer device. This is different from the other transformer based topologies and is recognizable from the polarity dots on the transformer that are reversed from primary to secondary windings.

When transistor Q_1 turns ON, the output diode will be reversed biased so no output current will flow. The transformer can only function like an inductor and store the energy in the primary winding. While the transistor is ON, the entire load current is supplied by the output capacitor C_{out}. When transistor Q_1 turns OFF, the current can no longer flow through the primary winding. The collapsing magnetic field reverses voltages on the windings. The diode D_1 is forward biased, and the current flows from the secondary winding through the diode and to the load and the output capacitor. The duty cycle should be less than 50% to prevent unstable operation. The input to output voltage transfer function is more complicated than most other topologies. The design of the transformer is significantly more complicated because its energy storage functionality.

MATERIALS AND METHOD

Design Implementation

Figure 3 shows the block diagram of the design set up. The input is usually high voltage and low frequency AC supply that available on wall socket. The first stage is a half wave rectifier and filter that convert the mains AC supply to DC voltage supply. High spikes and surge is being eliminated by the filter capacitor. The high voltage DC is controlled by high Frequency switching transistor that samples the high voltage DC with feedback path reference. Fly back ferrite core transformer step down the voltage as required, then followed by the second stage is rectifier and filter that gives constant DC output Voltage without current fluctuations.

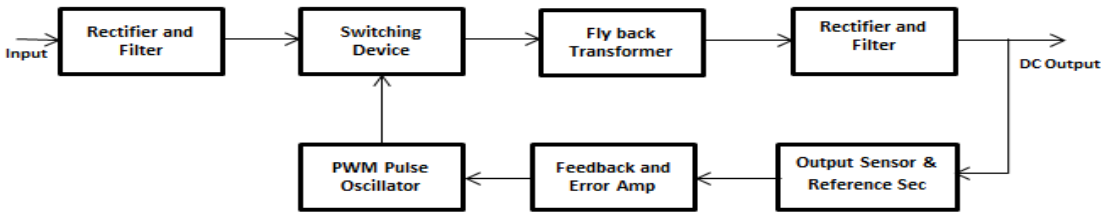

Figure 3: Block diagram of the design setup

Choice of the Switch Circuit

The self-oscillating fly back converter is designed to operate at theboundary of continuous and discontinuous conduction mode. It utilizes peak current mode control and operates with a variable switching frequency. The switch driver is implemented with a single transistor Q_2, a positive-feedback winding, and a resistor divider network. Switching action is performed by a high voltage and fast switching transistor. The switching transistor chosen for this study is MJE13003. It has 700V blocking capability and Inductive switching matrix 0.5 to 1.5 ampere at 25 and 100°C. It is recommended for switching regulator, inverters, motor control, relay drivers and deflection circuits (MJE13003 datasheet, 2014). The power supply is however required to works with universal input voltage supply of 85 to 265 V AC. It should be able to deliver a fairly stable output of full load within the range. For effective short circuit protection control UTC S8550 transistor is used in the design (Figure 4). The transistor also has collector emitter voltage V_{CEO} of 20 V and collector current up to 700 mA (UTC S8550 datasheet, 2014). It usually samples the voltage drop across a resistor (R_5) in series with switching transistor. If the current rises abnormally due to some shorted circuit or overload, the voltage will exceed the reference level and shutdown the pulse generator (Yusuf and Yahaya, 2020). In the bulk circuit FR107 switching diode was chosen due to its high current capability and low reverse current (FR107 datasheet, 2002). Feedback is implemented to retain the output voltage fixed with load line and variations – changes that occurs due to mains voltage and load. Zener diode and photocoupler were deployed for this function. The EL817 photocoupler is being use as a signal transmission between circuits of different potentials and impedances (EL817 datasheet, 2013). For this study it is a link between the two voltages. The value of C_1 was determined from the equation 1:

$$C = \frac{0.7(I_L)}{\Delta E(f)} \text{ (Jim, 2005)} \qquad (1)$$

Where C=capacitance in farads, I_L=DC load current in amperes, ΔE=peak to peak riffle voltage, f= ripple frequency (generally 100 Hz for full bridge and 50 Hz for half wave), 0.7 is the complement of the rectifier current duty cycle. Load current of 1mA and a ripple factor of 10% were assumed. Substituting I_L=1 mA and ΔE=10% of 85 V and had C_1=1.6 µF. 2.2 µF is closer standard is been used. For effective performance smoothing capacitor is usually chosen to be higher than the calculated value. R_1 is limiting the inrush current, in another word as a surge suppressor. In some power supplies thermistor is been used. For transistor Q_2 to operate its base emitter voltage (V_{be}) should be greater or equal to 0.7 V. The minimum input voltage (V_{in}) of the circuit was assumed to be 85 V while the base current (I_b) is 25 µA. From ohms law the biasing resistor R_2 found to be 3.4 mΩ. The standard value closer to it is chosen to be 3.6 mΩ. R_3 and R_4 limit the current through the base of transistor Q_2 and Q_1 respectively. Q_1 switches when the circuit is either overloaded or short-circuited. In an overloaded state voltage across R_5 will rise to 0.7 V and courses Q_1 to conduct. The emitter current (V_e) at this stage was assumed to be arrow 500 mA. R_6 and R_{10} limit the current passing through the photocoupler and LED respectively, while R_8 and R_9 in series provide a potential divider network. Lithium ion battery model LIR18650 has a minimum capacity of 2500mAh, discharge voltage of 2.75 V and nominal voltage of 3.7 V. It also needs a maximum charge voltage of 4.20±0.05 V and standard charge current of 0.52 A. (LIR18650, datasheet, 2010).

Ferric Transformer Design

The Transformer consists of two secondary windings: output winding and positive-feedback winding .The input power source is an AC 110 to 220 V main. Root mean square value (RMS) is about 311 V, while the frequency of the oscillator was chosen to be 100 kHz. To safeguard the battery (lithium ion) from over charging the final output voltage of the charger is expected to be 4.2 ±0.5 Volt, while the charging current is 0.5 to 1 A. The effective cross sectional area of the ferric transformer is already 3.7*3.7 mm. The circuit is expected to operate on universal input source of about 85 to 220 V, while the required output is also to stay fixed due to feedback circuitry.

Moreover Vin (max) = 220 V AC = (220 √2) V DC = 311 VDC, and Vin (nom) = 85 V AC = (85 √2) V DC is approximately equal to 120 V DC. From Faraday's Law:

$V=4.44NA_efB10^{-8}$ (Majid, 2009) (2)

Where; V is the applied potential (volts RMS), 4.44 is the form factor for a sine wave and 4.0 for square wave, N is the number of turns, A_e is the core effective cross-sectional area (cm^2), f is the frequency of the oscillation (hertz), and B is the peak flux density (gauss).

The great benefit of ferrites, of course, is that they permit operation at frequencies into the hundreds of kilohertz, even to several megahertz. With the frequency very high, A and N may be set to small values, and the resulting magnetic is miniature in comparison with a low frequency device. The number of required primary turns is calculated from equation 3 (Marty, 2005).

$$N_{pri} = \frac{V_{in}(nom)*10^8}{4*f*B_{max}*A_e} \quad (3)$$

Where: Npri is the number of required primary turns, Vin (nom) is nominal input voltage and A_e is effective cross-sectional area of the core in cm^2. The maximum flux density (B max) is taken to be in the range 1300G to 2000G. This will be acceptable for most transformer cores (Majid, 2009).

Oscillator's operating frequency was chosen to be 100 kHz, while Bmax was assumed to be 1500G. The effective cross-sectional area of the core is 13.69 mm^2. To the nearest whole number Npri was found to be 146 turns. The transformer output potential difference (PD) has to be greater than 4.2 V, due to voltage drop across the output rectifiers. Therefore, the transformer output must be [4.2 + (Total Voltage Drop Due to rectifier Diode)] at all input voltages. Hence, transformer output was rated at 6.0 V to compensate for this drop. To allow gap for the dead time, the pulse width modulation (PWM) controller was chosen to be 98% maximum duty cycle. At a maximum duty cycle of 98%, the average voltage to transformer is 0.98 * 120 V = 117.6 V. The ratio of primary to secondary is 117.6 V/ √2∗6.0 V = 13.86, which is the turns ratio (N). Therefore; Nsec = Npri / N = 146 / 13.86 is approximately 11 turns. For effective feedback axillary winding was also made to be 13 turns. The feedback path is archived by using an optocoupler EL817 integrated circuit and Zener diode. When the output DC voltage rises beyond the limit, the optocoupler gives a signal to the PWM transistor, and the PWM output pulse change accordingly.

The materials used in system construction were listed in Table 1.

Table 1: Materials used for construction

S/N	Component	Description	Quantity
1	Transistor	MJE13003	1
2	Transistor	UTCS8550	1
3	photocoupler	EL817	1
4	Zener D iode	1N4372A	1
5	Diode	1N14004	1
6	Diode	FR107	1
7	LED	Green	1
8	Capacitor	2.2 µF	1
9	Capacitor	470 µF	1
10	Capacitor	10 µF	1
11	Capacitor	4.7 nF	1
12	Capacitor	10 nF	1
13	Resistor	3.6 MΩ	1
14	Resistor	1 kΩ	2
15	Resistor	12 Ω	1
16	Resistor	10 Ω	1
17	Ferric core	13.69 mm^2	1
18	Resistor	560 Ω	1
19	Resistor	5.1 Ω	1
20	Resistor	2.2 kΩ	1
21	Resistor	3.3 kΩ	1
22	Resistor	1.2 kΩ	1
23	LED	Red	1

The circuit diagram prepared with "National Instruments NI MUTISIM", is presented in Figure 4.

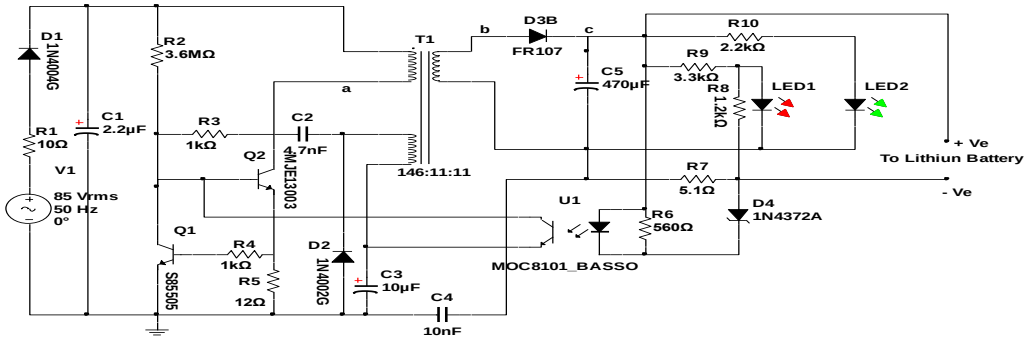

Figure 4: Complete Circuit Design

System Construction

All the components were first tested individually to determine their working conditions. Continuity test was accompanied for the transistors and diodes using a digital multimeter. The resistors were also found to be within their tolerance value. The tips of the components were thinned with lead for easier soldering. One after the other, the components was soldered to their places in the circuit. The active components, diodes and transistor were held by the pliers to help radiate the excessive heat quickly during the soldering. Primary winding of the transformer core done first, followed by the secondary and lastly the auxiliary. An insulation tape was used in between the windings. All the components were soldered on plane Vero board as shown in Plate 1.

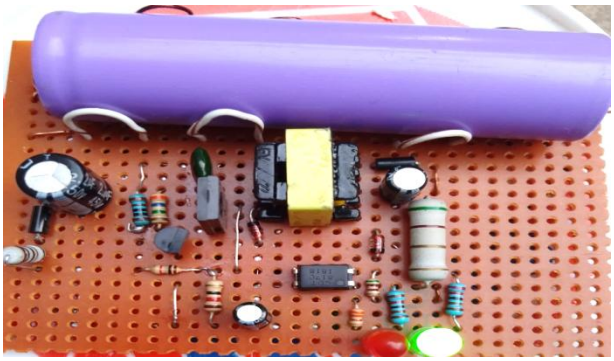

Plate 1: Photograph of the constructed circuit

RESULTS AND DISCUSSION

Simulations Test Results

Computer simulation test conducted at the oscillator output (point a), buck output stage (point b) and the final output of the whole circuit (point c) as shown in Figures 5, and 6.

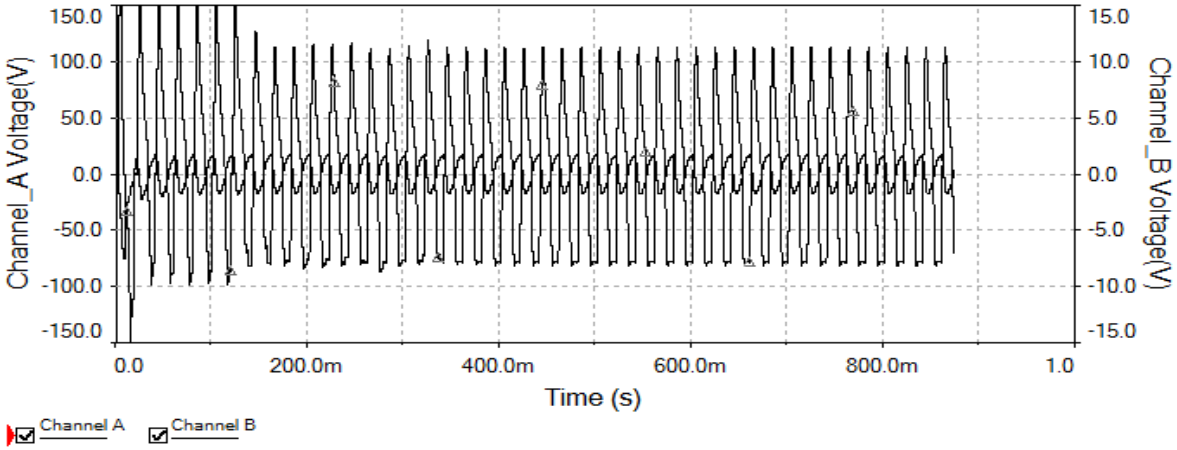

Figure 5: Analogue Simulations Test at point (a) and (b) in MULTISIM

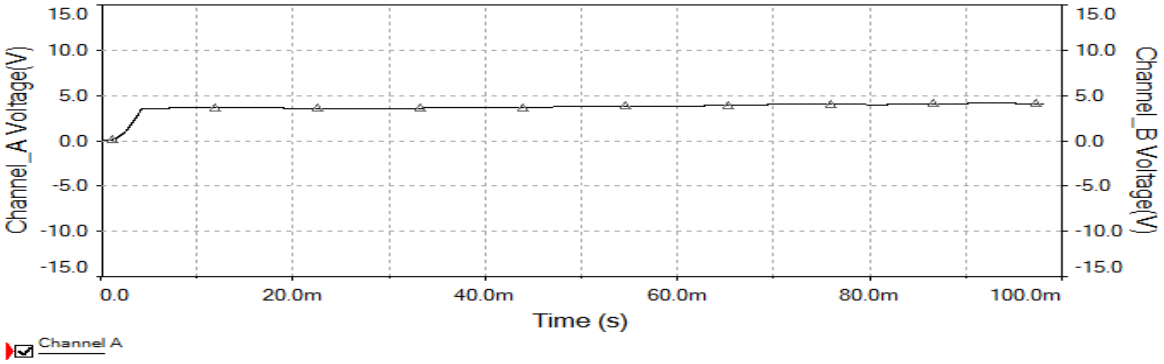

Figure 6: Analogue Simulations Test at point c in MULTISIM

Figure 5 shows the simulations test at point (a) and (b) that is square wave of random fluctuations in pins noise. Potential difference and frequency of the oscillation was also found to be fluctuating. The overall output of the Charger was found to be DC of about 4.11 Volt with small amount of ripples as shown in Figure 3.2. The main purpose of this work is to charge lithium battery directly; therefore extra filter circuit is not necessary. The Zener diode used in software design has Zener voltage (V_Z) of 3.0 V. During implementation process the Zener diode of V_Z 3.1 V was used. Simulation result shows that the circuit is working as projected.

System Tests

After construction, the charger output found to be 4.22 V DC in an open circuit. The circuit maintained the 4.22 V for the input supply of 85 to 220 volt. A cylindrical lithium ion battery (18650) was connected for test charging. The charger was plugged in to AC supply of about 220 V. Digital voltmeter was connected across the battery terminals and another digital ammeter in series to the charger output. The red LED indicator was ON showing that charging is in progress. Current and voltage during charging were observed at 30 minutes intervals for a period of three hours thirty minutes. The observations were tabulated and presented graphically as shown in Figure 3.3a and 3.3b. After a while the green LED light was ON, which is an indication that the battery is fully charged. The battery was removed from the charger and its PD measured and found to be 4.2V.

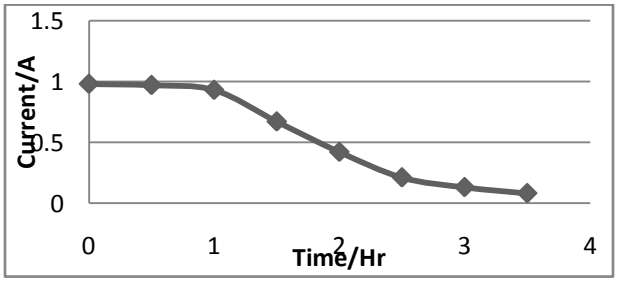

Figure 3.3a: Battery Charging Current VS Time

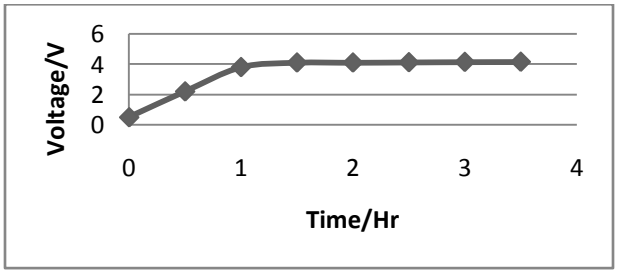

Figure 3.3b: Battery PD against Time

Figure 3.3a shows the charging current is decreasing non-linearly to around zero level. But the PD across is gradually increases till it reaches a peak value of 4.2 V with a very small increment toward the peak level as shown in figure 3.3b. In an overloaded stage, current developed will course transistor Q_1 to conduct as a result the base of transistor Q_2 will be grounded. Hence shutdown the pulse generator and protect the circuit from being damage.

CONCLUSION

The charger was found to operate on universal input voltage range of 85 V AC to 220 V AC. An output of 4.22 VDC was obtained within the range. It is suitable for charging lithium battery. Red LED is ON during charging while the Green LED indicator is ON to shows that the charging is completed. From the test and analysis conducted the charger was found to be working adequately.

REFERENCES

Alex, D. (2008). Introduction to Switch Mode Power Supplies, Microchip wave seminar, [Online] Retrieved Feb 11, 2018 from: http://www.microchip.com

Christine, Y. (2011). Simple Circuit Charges Lead-Acid Batteries, Application Note 621, Maxim Integrated, Retrieved from: http://www.maximintegrated.com/an621

EL817, Datasheet (2013). 4 pin DIP phototransistor photocoupler, Ever Light Corporation, [Online] Retrieved from www.everlight.com

FR107, Datasheet (2002). Fast Recovery Rectifier Diode EIC Dig Chip, [Online] Retrieved from http://www.digchip.com

Francisco, O., Ronald Q., Constantino, M., and Soriano, P. (2019). *International Journal of Innovative Technology and Exploring Engineering* (IJITEE) ISSN: 2278-3075, Volume-9 Issue-2, December 2019

Jim, K.(2005) Calculate Rectifier Input Capacitors, [online] Retrieved 15 Sep 2019, from https://www.electronicdesign.com/technologies/analog/article/21774995/confidently-calculate-rectifier-input-capacitors

Joe, L. P., Sasirekha, S., Naveen, D. K. D., Revanth, P.S. (2018). Working model for mobile charging, using wireless power transmission. *International Journal of Engineering and Technology* 7(3.12):548 DOI:10.14419/ijet.v7i3.12.16434.

LIR18650, Datasheet (2010). Lithium ion battery, EEMB Co., Ltd., [online] retrieved 19 Sep 2020 from http://www.eemb.com

Majid, D. (2009). From Powder to Transformer, Fairchild Semiconductor Power Seminar (2008-2009), p. 2.

Marty, B. (2005). Publication Order Number AND8039. ON, Semiconductor Components Industries, LLC, [Online] Retrieved Jan, 3 201 Retrieved from http://onsemi.com

MJE13003 datasheet (2014).*NPN Silicon Transistor*, Unisonic Technologies Co., Ltd, [online] retrieved 17 Sep 2020 from www.unisonic.com.tw

Odia O. O., and Okpor J. (2017). Design and Implementation of a Microcontroller-Based Adjustable Voltage Automatic Battery Charger, *Nigerian Journal of Technology* Vol. 36, No. 4, October 2017, pp. 1226–1232. Electronic ISSN: 2467-8821.

Ovbiagele, U. and Jerome, D. K. (2017).*International Journal of Scientific Engineering and Research* (IJSER) ISSN [Online]: 2347-3878 Index Copernicus Value (2015): 56.67 | Impact Factor (2017): 5.156

Udezue, C.U., Eneh, J., Unachukwu A., Onyemelukwe I., and Onyeka, H., (2016). 12V Portable Battery Charging System, *Pacific Journal of Science and Technology* 17(1): 5-11. May 2016

UTC S8550 Datasheet., (2014) low voltage high current small signal PNP transistor, Unisonic Technologies Co., Ltd, N [Online] Retrieved Feb 11, 2018 from: http://www.unisonic.com.tw

Yusuf, Y. & Yahya, H N., (2020). Design, Construction and Evaluation of 5A AC-DC Portable Lead Acid Battery Charger with an Inbuilt Automatic Shut OFF. *International Journal of Science for Global Sustainability* Vol. 6(2) July, 2020, pp. 126-134.